ACCURATE FIELD LEVEL AND PHASE CONTROL AND MONITORING FOR A PROTON LINEAR ACCELERATOR

K. Batchelor and G. Gallagher-Daggitt.
P.L.A. Division, Rutherford High Energy Laboratory,
Chilton, Didcot, Berks.

A method of setting up and maintaining the correct phase and amplitude of the fields in the three accelerating cavities of the Rutherford Laboratory Proton Linear Accelerator is described. A system using a shunt regulator valve to control the field amplitude during the 200 μsec beam pulse is presented and the effect of source impedance on the build up of power in an accelerating cavity discussed. Measurements taken on the P.L.A. are given for comparison with the theoretical results.

1. Introduction

The energy required by each proton in a proton linear accelerator is determined precisely by the radio frequency amplitudes and phases in the accelerating cavities of the machine, which that proton experiences. A beam of protons must necessarily be injected over a range of phases, but the inter-tank phases and the amplitude in each tank can be closely controlled. By doing so the stability of the mean energy and the energy spread of the beam can be optimised. Methods of setting-up and controlling each cavity individually and of monitoring the inter-tank phases on the Rutherford Laboratory P.L.A. are described. The amplitude and phase of the R.F. in the cavities has been calculated for the equivalent lumped tuned circuits, containing L, C and R, and these have been compared with the measured parameters of the 400 μsec pulse.

2. The Radio Frequency System

The block diagram, figure 1 shows the main components of the R.F. system[1], and Table I gives relevant r.f. parameters. The following units are of particular relevance to the discussion in section 3.

Table I. Radio-frequency parameters of the P.L.A.

	TANK 1	TANK 2	TANK 3
Unloaded Q value	85,000	64,000	47,000
Peak r.f. power	450 kW	1200 kW	1350 kW
R.F. pulse length	400 μsec	375 μsec	375 μsec

Operating frequency = 202.5 Mc/s, p.r.f. = 50/sec

a) The Standard Frequency Source consists of a 2.5 Mc/s crystal controlled oscillator with a stability of 1 in 10^8 and a series of frequency multiplying stages, giving an output of 5 watts at 202.5 Mc/s.

b) The GGT Amplifiers are grounded grid triodes with internal grid and anode tuned circuits. The output impedance of the triodes is not correctly matched to the coaxial line; it can be adjusted by anode cavity tuning and by a stub on the output line. The triodes are constructed by A.E.R.E. and the Rutherford Laboratory.

c) The Power Dividing Networks provide a means of adjusting the amplitude and phase of the r.f. drive to the final amplifiers, to obtain the desired phasing of the accelerating cavities and to obtain the necessary phases at the power combining network.

d) The Output System of the GGTs The anode stub and anode tuning are adjusted to give best power transfer into a matched load. The phase shifters are adjusted to optimise the transferred output impedance at the loop terminals of the cavities.

3. Powering of the high Q accelerating cavities

The provision of adequate r.f. power is one of the major cost items in proton linear accelerators, so it is desirable to minimise the cavity build-up time and to maximise the beam pulse length in a given system. Furthermore it is desirable to minimise the energy fluctuations in the output beam, which means that the amplitude and phase of the voltage in the cavities should be kept very constant. Ideally the amplitude should not vary more than a few tenths of a per cent and the phase by more than half a degree in order to achieve a mean output energy tolerance of 0.1% and an output energy spread of 0.2 to 0.3%.

Of the several factors contributing to the rise time constant and phase change during the voltage pulse in the cavity, the effects of source admittance and cavity tuning are investigated here for the case of a cavity powered by a current generator. The fundamental wave $I\sin\omega t$ only is considered, and the equivalent circuits and symbols of figure 2 used for the computation.

The basic differential equations for these two circuits are:-

$$\frac{d^2V}{dt^2}+\left(\frac{1}{CR}+\frac{n^2}{CR_s}\right)\frac{dV}{dt}+\left(\frac{1}{LC}+\frac{n^2}{L_sC}\right)V=\frac{I\omega\cos\omega t}{n} \qquad (1)$$

where the transferred source susceptance is inductive and

$$\frac{d^2V}{dt^2}+\left\{\frac{1}{(C+n^2C_s)R}+\frac{n^2}{(C+n^2C_s)R_s}\right\}\frac{dV}{dt}+\frac{V}{L(C+n^2C_s)}=\frac{I\omega\cos\omega t}{n} \qquad (2)$$

where the transferred source susceptance is capacitive. Equations (1) and (2) may be written as

$$\frac{d^2V}{dt^2}+\frac{\omega_o}{Q_L}\frac{dV}{dt}+\omega_o^2\left(1+\frac{n^2L}{L_s}\right)V=\frac{I\omega\cos\omega t}{n} \qquad (3)$$

and

$$\frac{d^2V}{dt^2}+\frac{\omega_o}{Q_L\left(1+\frac{n^2C_s}{C}\right)}\frac{dV}{dt}+\frac{\omega_o^2V}{1+\frac{n^2C_s}{C}}=\frac{I\omega\cos\omega t}{n} \qquad (4)$$

The solutions to (3) and (4) are

$$V = V_o\left\{\sin(\omega t+\alpha) - ke^{-mt}\sin(\omega' t+\beta)\right\} \quad (5)$$

where V_o, ω', α, K and β are defined in figure 3.

It can be seen from equation (5) that the rate of rise of voltage in the tuned circuit will depend upon the value of the transferred source susceptance and conductance and also upon the difference between the resonant frequency ω_o of the tuned circuit and the driving frequency ω. The phase of this voltage with respect to the driving current will also depend upon the value of these parameters. Also, since the modified frequencies ω_L or ω_C are not generally equal to the resonant frequency or the driving frequency there will arise a modulation of the voltage "build up", which may lead to a faster rise time than expected from a simple theory, which neglects the effects of source admittance. This effect has been observed on the P.L.A. and on other machines using an amplifier to drive a resonant cavity. Beam loading effects have been omitted from the calculation for simplicity. The phase response will now be considered in more detail.

For a given source admittance and cavity tuning equation (5) has V_o, K, m, α, β, ω and ω' all constants.

The vector diagram of figure 3 then represents this equation at one of the instants when $\omega t = 2p\pi$ (p=1,2,3...). The phase of V with respect to V_o can then be obtained:-

$$\frac{kV_o e^{-mt}}{\sin\theta} = \frac{V_o}{\sin\{(\beta-\alpha)+(\omega'-\omega)t-(180+\theta)\}}$$

Hence

$$\tan\theta = \frac{ke^{-mt}\sin\{(\beta-\alpha)+(\omega'-\omega)t\}}{ke^{-mt}\cos\{(\beta-\alpha)+(\omega'-\omega)t\}-1} \quad (6)$$

Typical theoretical and practical curves for Tank 1 of the P.L.A. are plotted in figure 4 where the effect of powering the cavity both on and off "resonance" is shown. For the inductive and capacitive cases the theoretical curve corresponding to $\omega = \omega_o - \omega_o/2Q_L$ (i.e. a driving frequency of 202.5 Mc/s $-^{o}240$ c/s) fits the practical curve well for the last 300 μsec of the 400 μsec pulse. The method of phase measurement used was not accurate for the early part of the pulse due to the large changes in cavity voltage over this region and changes in the source impedance also influences the result there. The values of Q_L used were calculated from the two measured build up curves corresponding to the practical phase curves given in figure 4. The measured phase change corresponds to the computed shift required to change the effective source reactance from $\omega_o L_s = 70.8\ \Omega$ to $1/\omega_o C_s = 83.7\ \Omega$.

It can be shown that for all practical cases the expression denoted by K in equation (5) reduces to 1 and that $\tan\alpha = \tan\beta$, so the effect of tank tuning is entirely due to the quantities $(\omega_L-\omega)$ or $(\frac{\omega_L\omega}{\omega_c}-\omega)$. Equation (5) may therefore be written as

$$V = \frac{I\omega\sin(\omega t+\alpha_L)}{nC\sqrt{(\omega_L^2-\omega^2)^2+(\frac{\omega_L\omega}{Q_L})^2}}\left[1-e^{-\frac{\omega_L t}{2Q_L}}\cdot\frac{\sin(\omega_L t+\alpha_L)}{\sin(\omega t+\alpha_L)}\right] \quad (7)$$

and

$$V = \frac{I\omega\sin(\omega t+\alpha_c)}{nC\sqrt{(\omega_c^2-\omega_c^2)^2+(\frac{\omega\omega_o}{Q_L})^2}}\left[1-e^{-\frac{\omega_L\omega t}{2Q_L\omega_c}}\frac{\sin(\frac{\omega_L\omega}{\omega_c}t+\alpha_c)}{\sin(\omega t+\alpha_c)}\right] \quad (8)$$

Similarly the phase term may be written as

$$\tan\theta = \frac{e^{-mt}\sin(\omega'-\omega)t}{e^{-mt}\cos(\omega'-\omega)t-1} \quad (9)$$

It is evident from the foregoing that some means of adjusting the effective transferred admittance appearing at the cavity would be useful. On the P.L.A. the phase shifter (line lengthener) in the output line of each grounded grid triode amplifier serves this purpose. In figure 5(a) the percentage of the final voltage amplitude at a fixed time (~150 μsec) after commencement of build up has been plotted as a function of the position of this phase shifter for Tank 1 of the P.L.A. This shows that maxima occur at half wavelength intervals of movement of the phase shifter. The minima would occur at the same intervals. If the cavity was powered "on tune" and there was zero transferred source susceptance the minima and maxima would be separated by a quarter wavelength. It is also enlightening to investigate the phase changes during the last 250 μsec of the 400 μsec r.f. pulse as a function of the phase shifter movement. This result has been plotted in figure 5(b) where it can be seen that zeros occur twice for every half wavelength of the line lengthener; the relative spacing of the two zeros being dependent upon the cavity tuning and the source susceptance.

The optimum setting of the line lengthener is that which gives zero phase change during the beam pulse together with the shorter of the two build-up rates, thus minimising the beam energy spread while obtaining nearly the longest available pulse length.

4. Automatic control of the Accelerating Field

Stabilisation of the electro magnetic accelerating field in the linear accelerator resonant cavities is achieved by applying automatic control in two stages. A slow acting system operates on the modulator EHT power supply and maintains it's output constant to within ±1%. A second fast acting system maintains the field in the cavity constant to within ±0.1%. over the duration of the beam pulse. (See figure 1). The latter system is required to:-

a) Eliminate the effects of disturbances which would otherwise cause changes in beam current, mean beam energy and energy distribution (See fig. 6). Such disturbances arise from changes in or distortion on the pulse modulating voltage applied to the GGT r.f. power amplifier anode (Disturbance u_1), changes in the r.f. drive power to the GGT (disturbance u_2) and changes due to beam loading (disturbance u_3).

b) Increase the interval over which the accelerating field is within ±0.1% of the value required for stable phase acceleration of protons, and thus enable better utilisation of the r.f. energy supplied to the cavity resonator.

Three fast acting control systems operate independently so as to maintain constant accelerating fields in the three sections of the accelerator.

Principle of operation (See fig. 7)

Fast control is effected by means of a parallel regulator valve (Type RS1041W) which has anode and cathode electrodes connected to the corresponding electrodes of the GGT's which supply r.f. energy to a cavity resonator. The anode load impedance of the regulator valve is the internal impedance of a modulator (Z_o), which, when transferred to the secondary terminals of a pulse transformer of turns ratio N, appears in the anode leads as an impedance N^2Z_o. Changes of potential at the control grid of the regulator valve control the voltage developed across the impedance N^2Z_o, hence, the voltage applied to the anode of the GGT and, in turn, it's r.f. output power. The arrangement is made self adjusting by sampling the r.f. field in an accelerator resonant cavity and comparing the pulse envelope of the sampled voltage with a stable dc reference voltage. An actuating error which is the difference between the two is amplified and applied to the control grid of the normally non-conducting regulator value so as to correct for deviations from the desired accelerating field.

When the control amplifier is operating under median conditions and the control loop is closed, approximately 10% of the modulator pulsed power output is dissipated in the regulator valve. Under such conditions, variations of the accelerating field within the limits ±5% are controlled. The positive limit depends on the power available from the modulator in excess of that necessary to produce the r.f. field condition required for stable phase acceleration of protons.

The effectiveness and stability analysis of the system[2] is based on the information given on the system flow diagram fig. 8. Corrective networks which modify the overall system function are not shown.

The transfer functions relate to the following physical elements:-

G_1 and a part of G_2 - relate to the control amplifier. The other part of G_2 relates to the parallel regulator valve and its load impedance. G_3 relates the changes in GGT anode pulse modulation voltage to r.f. voltage output. G_4 relates the r.f. voltage in the feed-line to the cavity resonator to the peak accelerating voltage in the cavity resonator. G_5 is the r.f. voltage gain of the GGT amplifier and does not include any frequency dependent term. H_1 relates the peak accelerating voltage in the cavity resonator to that coupled at low level, detected and applied to the input of the control amplifiers.

Fig. 9 shows Log modulus and angle graphs of the elements of the control system and a composite plot for the complete system is shown in figure 10. Log modulus and angle plots of the correction network are shown dotted in figure 10. Similar results are obtained for the other sections of the accelerator. A table on figure 8 gives a summary of the low frequency modulus values of the transfer functions and the correction factors for the three sections of the accelerator. These results show that the system of automatic control described is capable of a high degree of precision without being unstable. The method was chosen in preference to others because it avoided having to modify the existing scheme of pulse modulators and r.f. systems, and could easily be rendered inoperative in the event of it's failure without seriously effecting operations.

5. Monitoring and Control of radio-frequency field level and phase

(a) Radio frequency field level monitoring

(i) Metering For measurement of power flow in the coaxial lines to and from the grounded grid triode amplifiers and the accelerating cavities forward and reverse reflectometers are used. These measure mean power and are calibrated against power fed into a water load.

(ii) Control and interlock monitoring A signal from a small loop coupled to each cavity is detected by a silicon planar diode and after amplification and integration displayed on a milliameter. This unit also switches in the automatic cavity tuning system and the slow E.H.T. stabilisers of the G.G.T. amplifiers at 25% and 50% respectively of the operating field level.

(iii) Precise radio frequency field level monitoring Biased diode detectors are used to display the difference between a stable d.c. reference voltage and the radio frequency signal from a small coupling loop in each cavity. The small difference pulse representing 2% of the total radio frequency pulse is monitored on a C.R.T. and maintained constant to within ±5% giving an overall accuracy of better than ±0.1%.

(b) Phase Monitoring and Control[3]

An automatic phasing system is necessary to maintain a constant output spectrum from the machine. The system used for each cavity is shown in schematic form in figure 10. Each cavity is maintained "on tune" so that the final amplifiers always operate under the same "match" conditions. A forward reflectometer in the feed line to each cavity provides the phase reference signal whilst a monitor loop in the cavity itself gives a signal for comparison in a four arm bridge used as a phase comparator. The error signal from this bridge is used after suitable gating and amplification to drive a motor which in turn moves the tank tuners via a cam operated hydraulic system.

The system has a small "dead zone", an r.f. phase error of 0.04^o will produce full standard torque at the motor shaft, and the velocity lag

is 0.17 deg. degree^{-1} sec^{-1}. The maximum correction speed is approximately 16° sec^{-1}.

This system can allow drift in phase between accelerating cavities, due to changes in phase in the drive lines and the G.G.T. amplifiers. Hence a separate phase monitor system, which monitors phase during the 400 μsec r.f. pulse, is provided between each cavity and a common point in the drive system. Any drift in phase can be corrected by adjustment of the appropriate remotely controlled, motor driven phase shifter in the Power Dividing network. The phase detection system used is similar to that used for auto tuning and is capable of detecting phase changes of 0.1 degree.

6. Conclusion

A method of setting up and maintaining the correct accelerating fields in the Rutherford Laboratory P.L.A. has been described and practical results presented. Agreement between the simple theory presented and the practical results is good, particularly during the last part of the r.f. build up where the source impedance should be nearly constant. The cavity field stabilisers have been shown to maintain the accelerating field constant to within ±0.1% during the beam pulse and a method of maintaining the phase constant to within ±0.5 degrees over this region has been formulated.

7. Acknowledgements

The authors wish to thank Mr. L. Goodall for carrying out calculations on the response of the cavity field stabilisers, and Mr. J. M. Dickson for useful discussions.

8. References

1. K. Batchelor, "The P.L.A. of the Rutherford Laboratory" Conference on Linear Accelerators for High Energies at Brookhaven National Laboratory, August 1962.
2. G. Gallagher-Daggitt, "Automatic Control of the E.M. Field in a Proton Linac", Rutherford Laboratory Report NIRL/R/76.
3. J. J. Rockett "P.L.A. Progress Report 1964", page 13, Rutherford Laboratory Report NIRL/R/81.

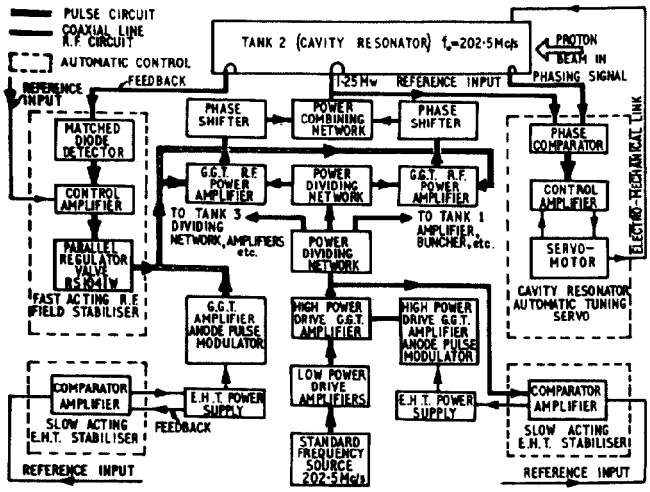

Fig. 1. Simplified schematic diagram of a section of the P.L.A.

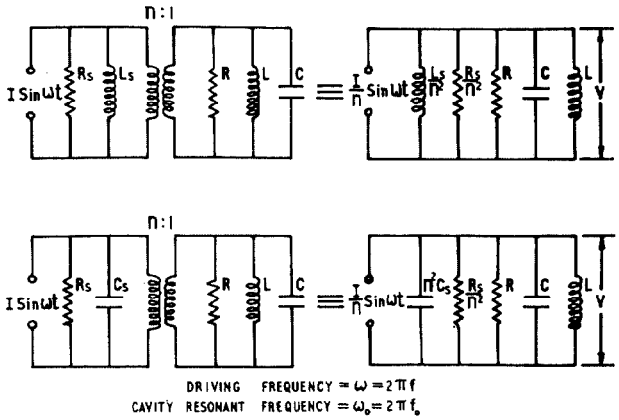

Fig. 2. Basic equivalent circuits.

$$\tan\theta = \frac{K e^{mt}\sin\left[(\beta-\alpha)+(\omega-\omega)t\right]}{K e^{mt}\cos\left[(\beta-\alpha)+(\omega-\omega)t\right]-1}$$

WHERE THE SYMBOLS ARE DEFINED BELOW FOR THE TWO CASES

INDUCTIVE CASE	CAPACITIVE CASE
$K=\sqrt{\dfrac{(\omega_L^2-\omega^2)^2+(\omega_L^2+\omega^2)^2\left(\frac{\omega_0}{2Q_L\omega_L}\right)^2}{(\omega_L^2-\omega^2)^2+\left(\frac{\omega\omega_0}{Q_L}\right)^2}}$	$K=\sqrt{\dfrac{(\omega_c^2-\omega_0^2)^2+\left\{\frac{\omega(\omega_c^2+\omega_0^2)}{2Q_L\omega_c}\right\}^2}{(\omega_c^2-\omega_0^2)^2+\left(\frac{\omega\omega_0}{Q_L}\right)^2}}$
$m=\dfrac{\omega_0}{2Q_L}$	$m=\dfrac{\omega_0}{2Q_L}\left(\dfrac{\omega}{\omega_c}\right)^2$
$\tan\beta=\tan\beta_L=\left(\dfrac{\omega_L^2-\omega^2}{\omega_L^2+\omega^2}\right)^2\dfrac{2Q_L\omega_L}{\omega_0}$	$\tan\beta=\tan\beta_c=\left(\dfrac{\omega_0^2-\omega_c^2}{\omega_0^2+\omega_c^2}\right)\dfrac{2Q_L\omega_c}{\omega}$
$\tan\alpha=\tan\alpha_L=\left(\dfrac{\omega_L^2-\omega^2}{\omega\omega_0}\right)Q_L$	$\tan\alpha=\tan\alpha_c=\left(\dfrac{\omega_0^2-\omega_c^2}{\omega\omega_0}\right)Q_L$
$\omega'=\omega_L=\omega_0\sqrt{1+\frac{n^2L}{L_s}}$	$\omega'=\dfrac{\omega_0\omega}{\omega_c}=\dfrac{\omega_0}{\sqrt{1+\frac{n^2C_s}{C}}}$
$V_0=\dfrac{I\omega}{nC\sqrt{(\omega_L^2-\omega^2)^2+\left(\frac{\omega\omega_0}{Q_L}\right)^2}}$	$V_0=\dfrac{I\omega}{nC\sqrt{(\omega_0^2-\omega_c^2)^2+\left(\frac{\omega\omega_0}{Q_L}\right)^2}}$

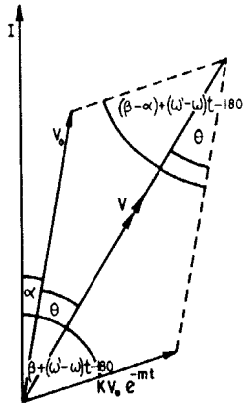

Fig. 3. Vector diagram and definition of symbols.

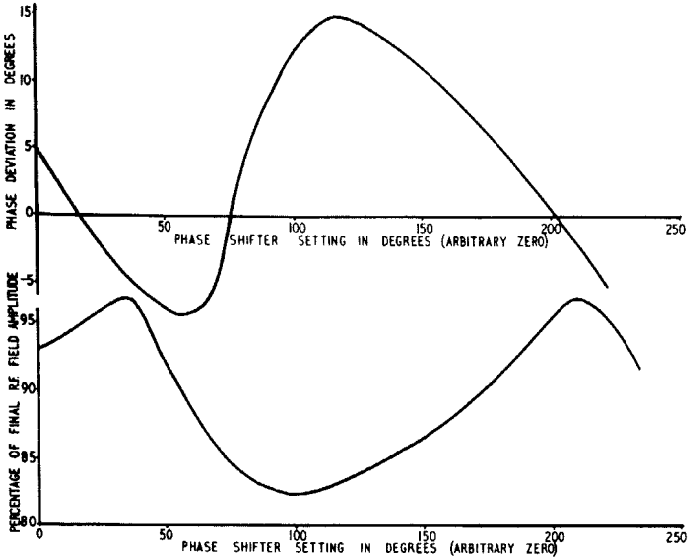

Fig. 5. Amplitude and phase response as a function of phase shifter setting.

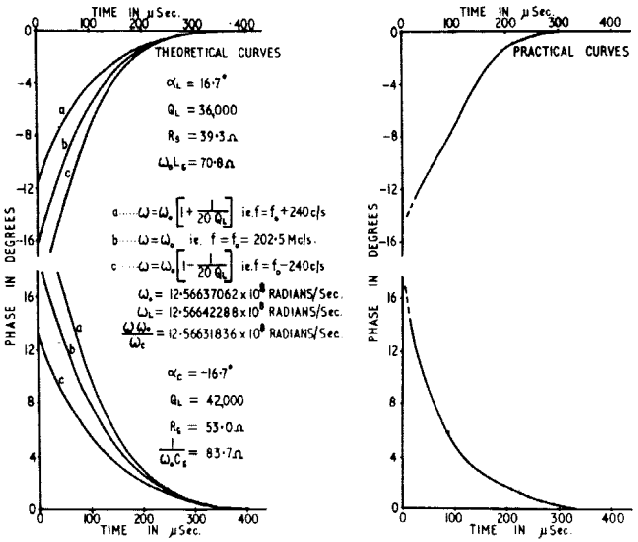

Fig. 4. Comparison between practical and theoretical phase response.

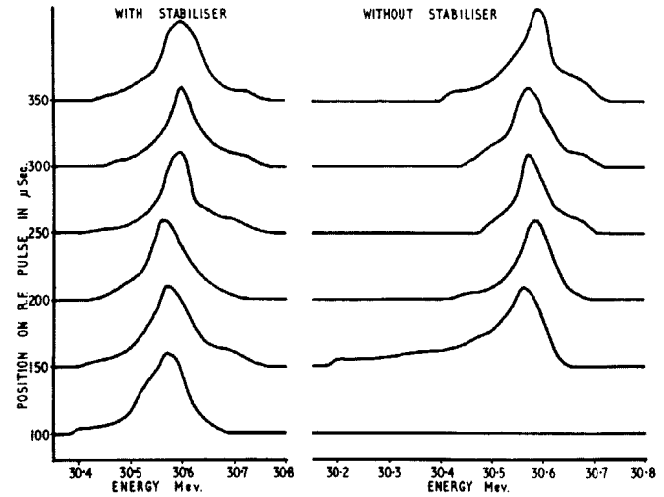

Fig. 6. Output spectra from Tank 2 taken with and without field stabilization.

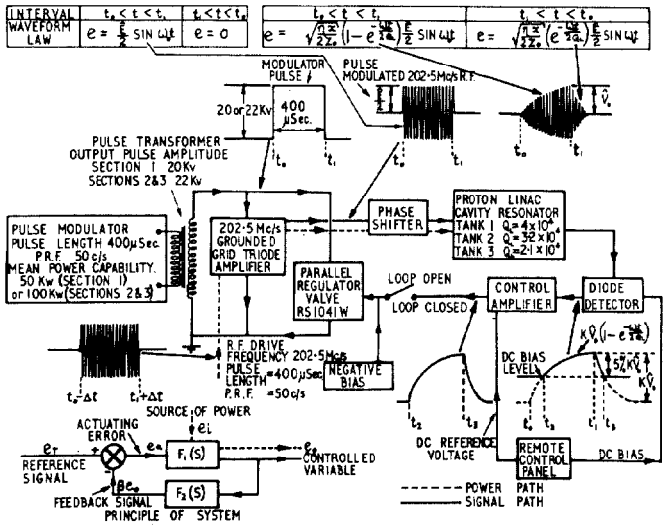

Fig. 7. Schematic diagram of the cavity r.f. field stabilizer.

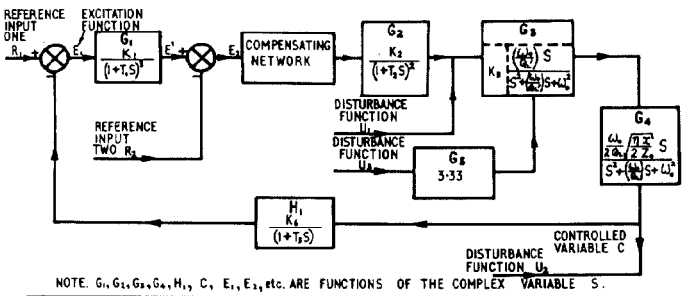

SECTION	η MEG-OHMS	X METRES	ω_0 Mc/s	Q_0	T_1	T_2	T_3	K_1	K_2	K_3	(1−H1G1) AT 50c/s
1	6·19x10³	5·94	202·5	4x10⁴	8/π x10⁴	27/π x10⁴	47/π x10⁴	138	1640	0·181	75·300
2	10·7x10³	11·95	202·5	3·2x10⁴	8/π x10⁴	27/π x10⁴	47/π x10⁴	138	1161	0·175	41·588
3	11·0x10³	11·24	202·5	2·1x10⁴	8/π x10⁴	27/π x10⁴	47/π x10⁴	138	1161	0·175	63·360

η = CAVITY RESONATOR SHUNT IMPEDANCE
X = CAVITY LENGTH
ω_0 = RESONANT FREQUENCY
Q_0 = CAVITY RESONATOR LOADED Q
Q_0' = G.G.T. R.F. AMPLIFIER ANODE CAVITY LOADED Q(40)
T_1, T_2, T_3 = CONSTANTS
K_1, K_2, K_3 = GAIN CONSTANTS
1−HG = CORRECTION FACTOR

Fig. 8. Field stabilizer system flow diagram.

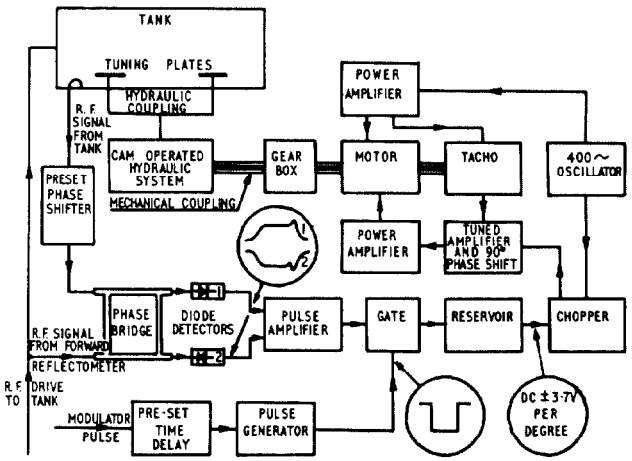

Fig. 11. The phase control system.

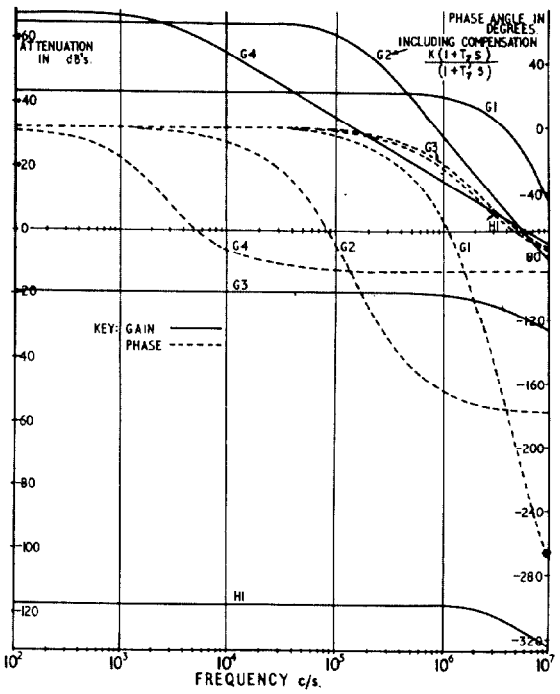

Fig. 9. Log modulus and angle plots of control system elements for Tank 1.

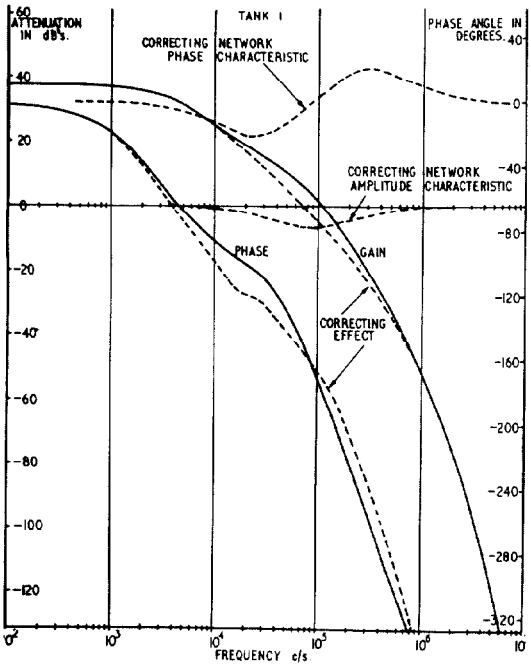

Fig. 10. Composite log modulus and angle plot of GH.